Proceedings World Geothermal Congress 2026
Calgary, Canada, June 8 – 11, 2026

Integrating Insights from Geological Mapping into Geothermal Conceptual Models

Nicholas Hinz[1]*, Ryan Libbey[2], William Cumming[3], Alex Milton[1], David Sussman[1], and Jill Haizlip[1]
[1]Geologica Geothermal Group, Inc., Reno NV, USA
[2]Ormat Technologies Inc., Reno NV, USA
[3]Cumming Geoscience, Santa Rosa CA, USA
*nhinz@geologica.net

Keywords: geothermal exploration, geological mapping, conceptual models, volcanic arcs, extensional settings, EGS, structural geology

ABSTRACT

Surface geological mapping provides key data inputs for geothermal conceptual models. To adapt methods to specific prospects, geothermal geoscientists benefit from understanding the similarities and differences in the application of surface geology mapping to geothermal prospects in disparate settings. To illustrate this, we compare geological mapping applications in volcanic arcs and active and passive extensional settings. We also address the application of geological mapping to the selection of EGS sites. In convective geothermal settings, surface geological mapping includes: documenting thermal manifestations and alteration to constrain the water table and evidence for hot and cold water flow; mapping faults and analyzing structural components that can constrain geothermal upflow, outflow and reservoir boundaries; mapping stratigraphy, unconformities and alteration to constrain the system's cap and outflow; and correlating lithology and alteration with geophysics. For EGS projects, surface geological mapping can inform the selection of favorable areas with lower structural complexity and provide insight into the local stress regime and stratigraphic framework. Geologic mapping to evaluate exploration and development risks is relevant to all types of geothermal systems. In volcanic settings, mapping volcanic fissures, domes and vents can indicate a heat source but can also indicate the disruption of the smectite cap, potentially indicating a risk of cool downflow. Where glaciation or a sector collapse has excised a smectite cap, cold water influx and/or permeability loss related to boiling and calcite deposition are potential risks. In extensional basins, permeable rock exposed in ranges adjacent to deep circulation geothermal systems commonly contribute to the artesian pressure of geothermal reservoirs and can provide a source of marginal recharge that can represent both pressure support and a cooling concern. In all these systems the host lithology can have a profound influence on chemistry that is important to its characterization and its production technology. Strategies surrounding surface geology mapping must be adapted to the local context of a project, and the implications of the results for the geothermal conceptual model are often best understood through analogue comparisons to other settings.

1 INTRODUCTION

Surface geological mapping provides fundamental insights into the components of geothermal conceptual models used to characterize resource potential and exploration risk. Hinz et al. (2024) detail standards for interrogating geological maps and producing new maps that meet the needs of geothermal project assessment and planning. This paper is intended as a tutorial and identifies typical applications of high-quality geological maps to the characterization of key geothermal conceptual model elements.

Surface geology mapping is an iterative process in geothermal exploration and development. The initial regional mapping informs more detailed local mapping, which in turn guides follow-on geophysical survey design and drilling targets. Subsurface data from exploration drilling efforts often prompt the need for further mapping to refine the geological model of a system. Probabilistic predictions of production and injection zones can be made more quantitative by checking which permeable zones encountered in wells are correlated with faults mapped at the surface (Stark et al., 2015). Similarly, borehole image logs can be used to characterize the reliability with which structures mapped at the surface can be projected into the subsurface. Although surface geology mapping is periodically revisited in geothermal fields for development planning and for the validation of predictions, the focus of this paper is on the use of surface geology mapping to build conceptual models during the initial exploration of a geothermal prospect.

A brief overview of surface geology mapping standards in geothermal exploration includes the regional geologic characterization that provides the context for the overall assessment. This helps identify the geothermal play

types that might be found, the geoscience methods and strategies that are likely to be effective in identifying and exploring prospects, and the developed geothermal reservoirs that might serve as appropriate analogues. Because of the importance of fracture permeability in convection-dominated geothermal systems, the reliable interpretation of local structural geometry is emphasized, with examples illustrating both structural reservoir targets and the common situation where the most reliably mapped structures characterize reservoir boundaries, rather than permeable targets. A resource and/or well targeting decision framework can be based on key structural settings identified from geological mapping (e.g., Faulds and Hinz, 2015). Recognizing and documenting uncertainty in mapped fault kinematics and geometry is essential to making structural mapping effective in geothermal assessments. Stratigraphy is sometimes underemphasized in geothermal conceptual models despite its role in identifying effective host rocks for targeting fracture permeability. In some geothermal reservoirs, matrix permeability can dominate over fracture-based permeability, for example, in geothermal systems hosted in karstic carbonates. Lithology also plays an important role in hosting, and potentially disrupting, the smectite cap of a system. Identification of high rank relict alteration (e.g., propylitic) at the ground surface can complicate delineating the details of the cap and reservoir in exploration of the modern geothermal system. Although geothermal exploration efforts commonly focus on the characterization of hot upflow and outflow, the downflow of cold water in fissures, domes, and vents that disrupt the clay cap can have profound effects on the size and temperature of a geothermal resource. Surface geology mapping can constrain the likelihood of chemistry risks associated with a resource that might be influenced by acidic, hypersaline or high gas zones. Therefore, surface geology mapping can provide an initial low-cost assessment of many conceptual model elements and risk issues including upflow/outflow/downflow zones, the cap, boundaries, chemistry risks, drilling concerns, and implications of sector collapse in volcanic systems.

This paper reviews geological map interpretation strategies across tectonic settings and among different geothermal system types. Case histories are outlined to illustrate lessons learned for the application of geological mapping to geothermal exploration and development. Some sections of the paper are supported with figures; however, the paper is largely supported by numerous references to manage overall length. Future papers are planned to cover subtopics cover in this paper with expanded figures to complement the text.

2 GENERATING HIGH-QUALITY GEOLOGICAL MAPS AND CROSS-SECTIONS

Best practices of geologic mapping programs for geothermal applications are addressed in companion tutorial paper by Hinz et al. (2024). The key components to the workflow, focus, and products are summarized to provide context for the examples in this paper. The workflow for generating maps for geothermal projects begins with reviewing the regional geological setting, the type(s) of geothermal resources that are likely to be present, and the existing geological map data. This helps define the map area and objectives of the mapping project directed at establishing a geological context for the information that first focuses attention on a local prospect.

The mapped area should encompass the stratigraphic and structural framework relevant to the prospective geothermal system, typically extending several times beyond the anticipated resource footprint to include both potential upflow and outflow regions. A mapping scale of approximately 1:25,000 generally provides sufficient resolution to capture fault geometry and stratigraphic contacts, although localized features such as surface manifestations may require more detailed mapping scales (e.g., 1:2,000).

A high-quality geologic map for geothermal exploration should clearly define, symbolize, and attribute the following elements:

- the stratigraphic framework, which delineates lithologic units, contacts, thicknesses, and compositional variations supported by field measurements where possible;
- the structural framework, which characterizes fault geometries, kinematics, and relative ages, with emphasis on Quaternary-active faults that may host or constrain geothermal fluid flow;
- alteration outlines or shading that document type, extent, and intensity to distinguish between active and relict systems based on detailed field observations; and
- surface manifestations and their associated deposits, including springs, fumaroles/steam vents/cold gas vents, mud pots, hot altered ground, travertine, and silica sinter, which should be mapped precisely to identify areas of active/recent geothermal activity.

Finally, cross-sections drawn perpendicular to the structural strike direction(s) should integrate geological, and other subsurface data when available (e.g., geophysical and well data) to effectively represent the three-dimensional subsurface framework controlling and constraining the geothermal resource, with particular attention to likely capping and reservoir rocks and using geophysics and drilled analogues to extrapolate from surface exposure to formations at depth.

3 INSIGHTS INTO GEOTHERMAL CONCEPTUAL MODELS FROM SURFACE GEOLOGICAL MAPPING

This discussion of the process of utilizing data from surface geologic mapping for the identification of key conceptual model elements of geothermal fields assumes that the geological maps have been generated through best practices, including capturing uncertainty in the surface observations.

3.1 Regional Geologic Context

This stage of data review typically includes using 1:>1,000,000 maps to gain an understanding of regional geology including regional tectonic settings and local neotectonics (crustal stress/strain conditions), volcanic setting (if applicable), lithospheric/crustal thickness and heat flow, and the presence/absence of surface manifestations. Paleogeographic reconstructions and models of regional geological history are also directly relevant for interpreting and predicting unit relationships in the field and elucidating the origins of structural trends. The context provided by regional-scale reviews provides a framework for understanding the likely ranges of resource characteristics and appropriate analogues for targeting a geothermal system.

The general questions that should be addressed with this regional-scale review are:

- *What is the geothermal province type?* e.g., is it situated within an oceanic or continental volcanic arc, an active or passive extensional setting, a region of post-collisional magmatism, a sedimentary basin, or a hybrid of these settings?
- *What is the predicted stratigraphy and regional structural context?*
- *What are the thermal gradient and heat flow characteristics of the region?* e.g., are mid- to upper-crustal heat sources possible/likely? Is the regional background (conductive) heat flow low (<~60 mW/m^2), moderate (~60-80 mW/m^2), high (~80-120 mW/m^2), or very high (>~120 mW/m^2)?
- *What are the regional crustal stress and strain dynamics?* e.g., Is the crustal stress regime expected to be extensional, compressive, or transitional, and how pronounced is the strain rate?
- *Are there direct lines of evidence for hydrothermal convection in the region?* Such as what is the distribution of surface thermal manifestations, hot wells, and/or developed geothermal systems in the region?

This regional understanding assists with the formulation of initial hypotheses and the focusing of exploration efforts at the field scale (1:<25:000) and provides important context for phenomena observed at the outcrop and hand lens scale during field mapping.

3.2 Structural Controls on Permeability

Faults shown on geological maps ideally illustrate a range of characteristics including, surface/subsurface trace, type of fault (normal, strike-slip, reverse, or thrust), recency (e.g., Quaternary active), and magnitude (length, offset, penetration depth). In addition to this, some faults or fault segments are mapped as concealed, which impacts certainty of the location or the extent to which they can be projected along strike. Other faults or fault segments, whether mapped as concealed or exposed may also be queried (labeled with question marks) and this impacts the certainty of interpretations as used in symbology by the USGS and other governmental geological surveys worldwide.

Most faults in geothermal areas can be expected to have a version of brittle fault zone architecture, except for old faults restricted to metamorphic rocks that had previously undergone ductile deformation below the brittle-ductile transition zone in the crust and have since been exhumed, or in surficial unconsolidated deposits. Brittle fault zones may act as conduits, barriers or both conduits and barriers relative to intrinsic qualities of the internal fault zone architecture and extrinsic controls, such as tectonic stresses and strain patterns (e.g. Caine et al., 1996; Rawling et al., 2001). Intrinsic qualities of fault zone architecture, including the textures and structures of the fault core and damage zone are controlled by protolith, displacement history, and fluid chemistry within the fault zone. These parameters vary between individual faults and along strike and down dip (e.g., Rapolano geothermal area, Italy; Brogi, 2008). As for extrinsic factors controlling fault zone permeability, research has shown positive correlation between greater regional strain rates (faults with higher slip rates) and the distribution of power-capable resources in the Great Basin region (Faulds et al., 2012; 2015) and in arc settings (Hinz et al., 2016). Furthermore, the majority of the power capable convective geothermal systems are associated with faults active in the latest Pleistocene to Holocene (Bell and Ramelli, 2007; Faulds et al., 2015; Hinz et al., 2016). With respect to tectonic stress, critically stressed fault segments are most likely to act as fluid flow conduits (Barton et al., 1995; Sibson, 1994; Townend and Zoback, 2000; Siler, 2023).

The brittle fault architectural features that contribute to permeability associated with faults and fault segments are associated with key structural settings. In the last three decades, significant advances have been made in recognizing the structural settings that are more likely to play a role in defining the location and geometry of geothermal systems in different geological contexts, including deep circulation systems hosted in extensional fault zones, magmatically-heated systems associated with arc volcanoes, and volcanic/magmatic rift-related systems (Curewitz and Karson; 1997; Rowland and Sibson, 2004; Fairley and Hinds, 2004; Micklethwaite and Cox; 2004; Rowland et al., 2012; Faulds and Hinz, 2015; Hinz et al., 2016, 2018; Faulds et al., 2006, 2009, 2011, 2013, 2021; Jolie et al., 2021; Faulds et al., 2026). These structural settings include pull-apart basins along strike-slip faults, displacement transfer zones where strike-slip and normal faults are linked kinematically, step-overs along normal faults, terminations of major normal faults, accommodation zones, and intersections of major faults (Figure 1). The tendency for geothermal fields to be more commonly associated with particular structural settings is complicated by the prevalence of the structural settings in different geological contexts. For example, deep-circulation geothermal systems in extension provinces are more commonly associated with the normal fault step-overs (B in Figure 1; Faulds et al., 2026) that are commonly found in that geologic context, whereas magmatically-heated fields below the flanks of arc-volcanoes are more commonly associated with transtensional pull-aparts (F in Figure 1; Hinz et al., 2016).

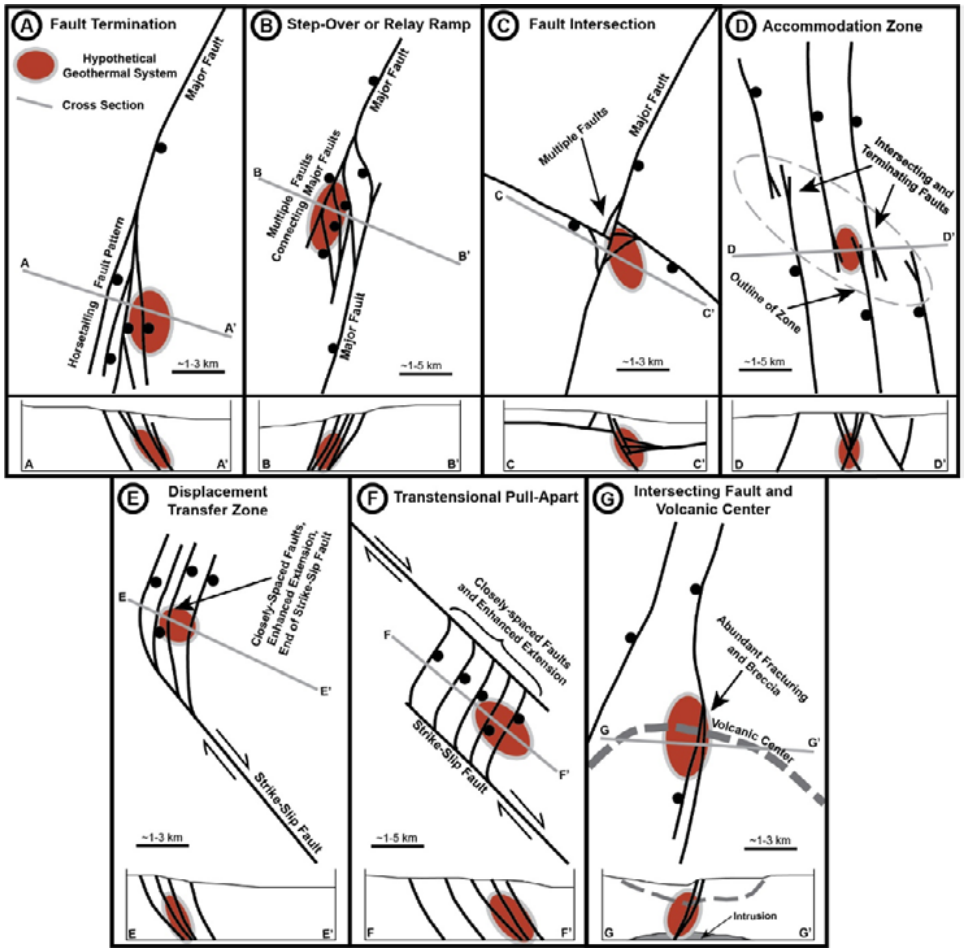


Figure 1: Schematic representations of favorable structural settings with accompanying cross sections (reproduced from Faulds et al., 2021). Red shaded areas mark approximate locations of hypothetical geothermal upwellings in map view and cross sections. (A) Fault tip or termination showing horsetailing pattern of closely spaced faults at the termination of a major normal fault. (B) Step-over or breached relay ramp showing abundant minor faults connecting overlapping strands of a major normal fault zone. (C) Fault intersection with abundant minor faults proximal to the intersection. (D) Accommodation zone (marked by gray ellipse) encompassing a belt of terminating, overlapping, and intersecting normal faults. (E) Displacement transfer zone whereby a major strike-slip fault terminates in an array of normal faults. (F) Transtensional pull-apart incorporating multiple closely spaced normal faults connecting a releasing step in a major strike-slip fault. (G) Intersecting normal faults with the margin of a volcanic center (thick dashed gray line).

Notable examples of key structural settings include published case studies of normal fault step-overs (B in Figure 1) in the Great Basin region, USA, e.g., Bradys and Desert Peak (Faulds et al., 2010) and Star Peak (Carver et al., 2021). In the western branch of the East African Rift Systems, the Panyimur and Kibiro geothermal areas in western Uganda are also hosted along step-overs (Hinz et al., 2018). Examples of displacement transfer zones where normal faults splay at the end of a strike-slip fault (E in Figure 1) include Blue Mountain and Don Campbell in the Great Basin region (Faulds et al, 2021; Hinz et al., 2024). Geothermal systems associated with terminations of major normal faults (A in Figure 1) include La Bouillante in Guadeloupe (Bouchot et al., 2010) and Salt Wells and Stillwater in Nevada (Hinz et al., 2014; Faulds et al., 2021), albeit the upflow for the latter two fields has yet to be fully characterized. Examples of fields associated with pull-aparts along strike slip faults (F in Figure 1) include Muara Laboh and Sorik Marapi in Sumatra, Indonesia (Mussofan et al., 2018; Stimac et al., 2019; Hinz et al., 2021; 2024) and the Salton Sea and Cerro Prieto geothermal systems in the Salton Trough along the San Andreas fault system. The most common settings include step-overs and pull-aparts, the dimensions of which range from about 200 m to 3 km across, with some larger examples spanning up to ~8-10 km across. Note that the scale of the structural setting can be smaller or larger than the productive reservoir area, however the upflow is rooted within the key structure.

3.2.1 Identifying Key Structural Settings

In exploration and development of resources, the practice of identifying and characterizing key structural settings has been demonstrated to be foundational to geothermal conceptual models, as the architecture of these guide upflow and outflow patterns. Most key structural settings are defined based on about two to five major faults. To identify key structural settings, it is necessary to distinguish at map scale the major faults relative to the lesser magnitude (minor) faults, along with their kinematics and information on recency (age). There is not currently a formal definition of *major* versus *minor* map scale faults in general geological mapping style guidelines. For geothermal geology, most of the major faults have strike lengths that are commonly several kilometers in length, have at least 100 m or more of offset (horizontal and/or vertical displacement), commonly have been active in recent (Late Quaternary) time, and can be identified by detailed surface mapping and/or through geophysics and well data. Major faults may define basinal or intrabasinal boundaries, or comprise the segments of major strike-slip faults (e.g., Sumatra Fault, Philippine Fault, or El Salvador Fault), or are newer developing late Neogene/Quaternary map scale faults that transects the geothermal area and are not yet bounding major basins or are part of a regional (e.g., >100 km long) strike-slip fault zone. Major faults can also include shorter segments that kinematically link major strike-slip or normal faults in pull-aparts and step-overs, respectively (B or F in Figure 1), or are major synthetic splay faults of a major fault but don't fully link with a second major fault. In some field areas, there are multiple generations of major faults, with some clearly younger and cross cutting the older set(s) of faults. In general, many minor faults are commonly synthetic or antithetic faults relative to the major faults. Field photos of examples of major and minor faults are shown in Figure 2.

An example of distinguished major and minor faults on a geological map is shown in Figure 3. This map is from the Bradys geothermal area, Nevada, USA. Power generation began in 1992 with average production for the past 8 years at ~10 MWe net. There is high quality publicly available detailed mapping (Faulds et al., 2017) and extensive published studies on this field such as Siler and Pepin (2021, references therein). The geological map by Faulds et al. (2017) is based on surface geological mapping, detailed lithology logs, 2D reflection seismic, and gravity data. The map (Figure 3a) includes numerous concealed faults, many of which have been defined through subsurface data and geophysics. The primary fault zone (Figure 3b), informally referred to as the Bradys fault zone in previous publications, is a west-dipping normal fault that hosts upflow within a ~250 m wide left step in this fault zone (Faulds et al., 2010). Outflow is structural-stratigraphically hosted and extends both north and south along the fault system from the upflow in the step-over, coincident with fumaroles and sinter deposits that extend for ~2.5 km along the fault zone both directions from the center of the step-over. Fumaroles developed at this field after production started, the liquid level and reservoir pressure dropped, and boiling commenced. Concealed west-dipping synthetic splays of the Bradys fault zone extend about 1 km west from the primary fault trace. Bradys fault zone abuts a horst block and all faults shown on the map to the east are east-dipping. Within the map extent in Figure 3, the Bradys fault is the only fault with Quaternary fault scarps, with the most recent rupture in the Holocene.

3.2.2 Key Structural Settings: Exploration and Development Project Phases

Based on these case studies, the structural setting and structural-stratigraphic permeability patterns for many geothermal systems are bounded and controlled by major faults or fault zones and hundreds to thousands of secondary faults and fractures, most of which do not have surface expressions. By using conceptual models that include the framework of these structural settings, successful geothermal wells can still be achieved by targeting favorable structural zones, even if the targeted regions are devoid of major mapped faults, as there are

often secondary faults that represent high permeability up-dip or along-strike splays of the major faults. As projects advance through the exploration and development phases, fault models should be updated, sometimes with major changes or additions, as new high-quality information is obtained from drilling data and image logs that provide 3D characterization of the major and minor faults. The conceptual models can also help to identify major faults that are not that can bound the edge of reservoirs where the fault core is impermeable, or there is a permeability contrast across the fault associated with juxtaposition of different rock units. Additionally, major faults can also be associated with cool crossflows adjacent to reservoirs, or downflows, particularly at basin margins such as at Blue Mountain, Nevada (Fercho et al., 2023) or Bweengwa, Zambia (Hinz et al., 2020).

Just as geological maps can be used to explore greenfield geothermal systems and contribute to the conceptual models for developing fields, the maps can also be used to identify areas suitable for EGS and AGS projects. Examples include recent and ongoing EGS proof of concept projects like Fallon FORGE, Utah FORGE, and Project Red (Fercho et al., 2023) and larger scale EGS projects (e.g., Project Cape; Fercho et al., 2025). All of these projects used existing geological maps and drilling data to target areas of lower structural complexity and predictable stratigraphy.

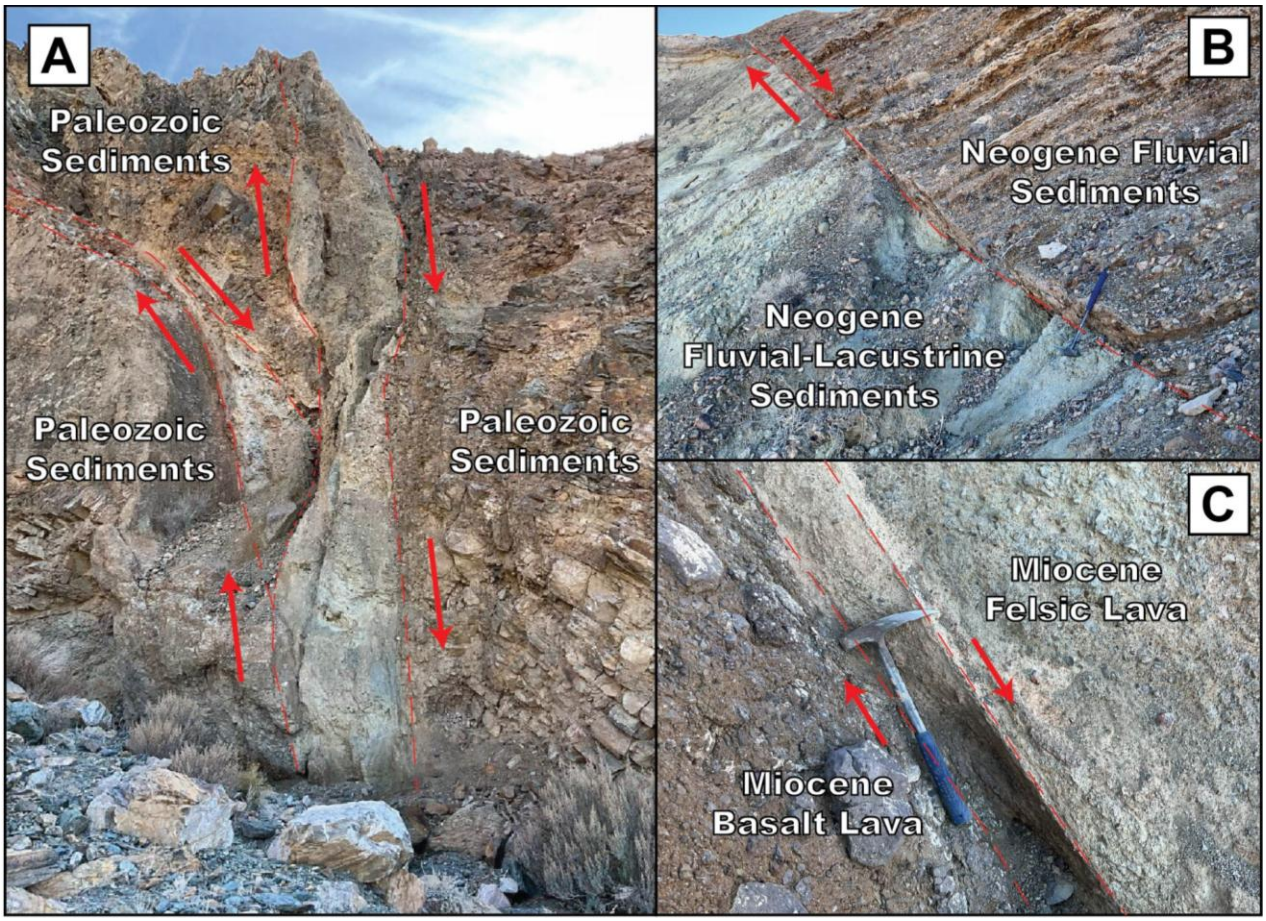


Figure 2: Examples of major faults. (A) Intersection of major fault splays, both within the footwall of a normal fault and within step-over. Width of the fault breccia core at the bottom of the hillslope is ~2 m. The splay on the right in the photo has an estimated 200 to 300 m of stratigraphic offset. This exposure is along a fault with >30 km length. The Paleozoic sediments are unaltered at this location. (B). Relatively major segment along a 5-8 km-long normal fault zone with >100 m of stratigraphic offset. Locally unaltered at this location. (C) Normal fault segment with ~150 m of stratigraphic offset and is ~3 km long, located within a normal fault step-over along a fault zone that extends 40 km long or more. Strata are unaltered in this outcrop. (A), (B), and (C) Outcrops are all located at separate geothermal project areas in Nevada, USA.

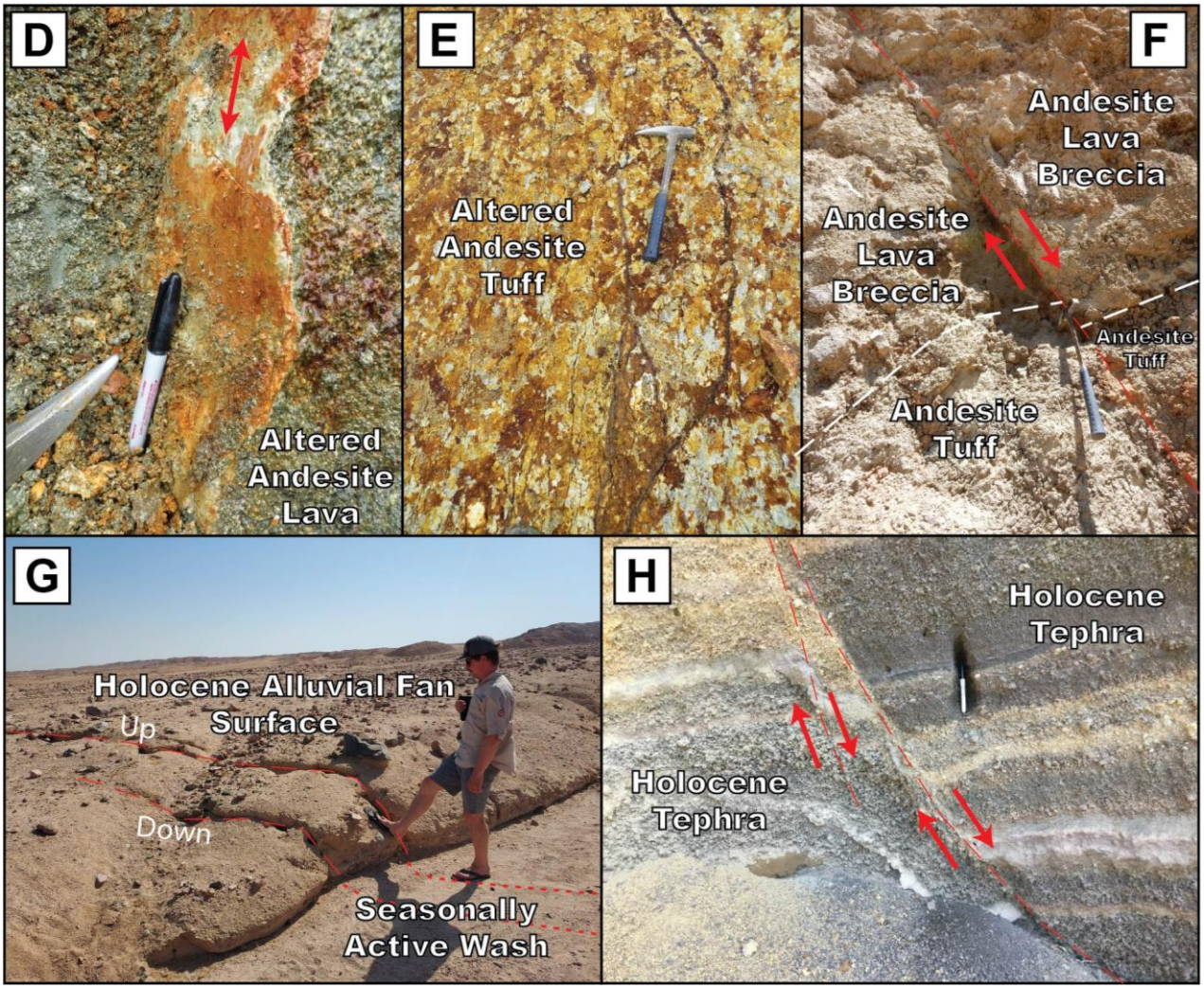


Figure 2 Continued: Examples of minor and major faults. (D) Akutan geothermal area, Alaska, USA: Minor outcrop scale fault (not map scale) with preserved kinematic indicators. Lithology is Pliocene to early Quaternary andesite lava. Located within a few hundred meters of a fumarole area, above the water table as defined by chloride springs, and in an area of discontinuous argillic alteration and oxidation exposed in the headwall area of a glacial valley. Hot Springs Bay Valley geothermal area, Akutan Island, Alaska, USA: (E) Minor outcrop scale fault (not map scale) without preserved kinematic indicators. Lithology is Pliocene to early Quaternary andesite tuff breccia. Located in an area of extensively exposed argillic alteration, oxidation, and silicification that is exposed in ridges north of the active Hot Springs Bay Valley geothermal area. (F) Minor fault with 15 to 20 cm of stratigraphic offset in argillic altered Quaternary andesite volcanics exposed in part of the exhumed cap of the modern geothermal resource at Sokoria, Flores, Indonesia (Hinz et al. 2020). (G) 10-20 cm scarp associated with 1995 earthquake rupture in the Gulf of Aqaba region of NW Saudi Arabia. Although small vertical magnitude, this surface rupture was mapped out for ~12km in length and locally aligned with older Pleistocene scarps with 10+ m heights, supporting that this qualifies as a major fault and could host a convective geothermal resource (Milton et al., 2023). (H) Minor fault with 0.5 m of displacement exposed in Holocene tephra within the Sokoria geothermal area, Flores, Indonesia. This amount of offset does not justify a map scale fault, either minor or major, however, this could be a relatively young (Holocene) surface propagation rupture from a larger magnitude fault in the subsurface. Features like this could be compared with up-dip projections of major faults if intersected and assessed with image logs from wells.

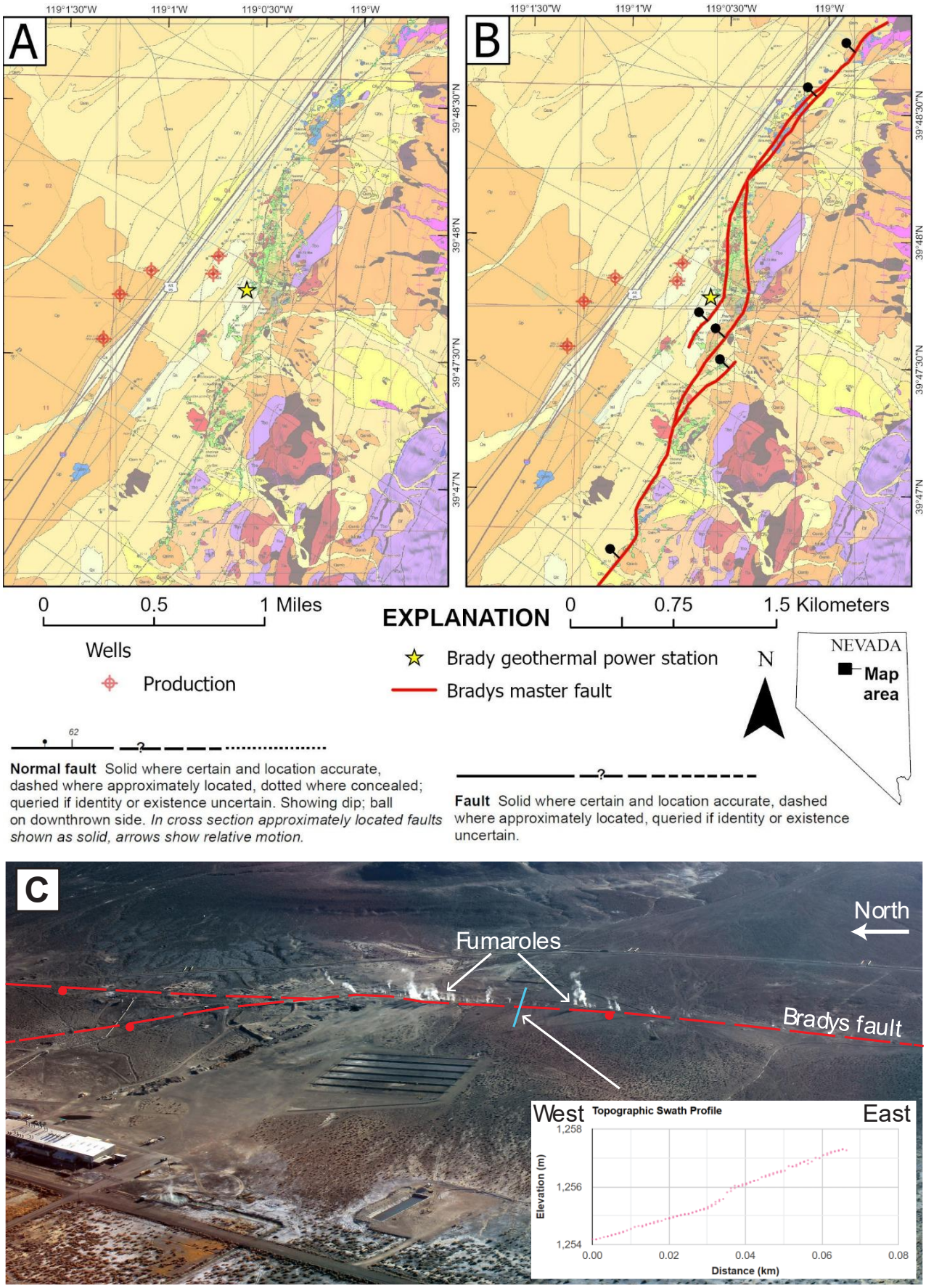


Figure 3: (A) Geological map of the Bradys geothermal area, Nevada, USA (Faulds et al., 2017). (B) Major fault segments of the Bradys fault zone shown in thick red lines. Detailed legend for the base map in each figure (A and B) can be found on Faulds et al. (2017). (C) Annotated photo of steam from fumaroles along the main Bradys fault trace south of the step-over. View is looking east. Photo credit to John Bell.

3.3 Lithological Permeability Controls and Influences on System Hydrology

The range of primary permeability values for rocks in the upper crust spans 14+ orders of magnitude (Wallis et al., 2015). It is thus expected that the distribution of lithologies with different primary permeability characteristics, in conjunction with structural permeability pathways profoundly influences the hydrology of geothermal systems. The interplay of fault/fracture and lithological controls of permeability in geothermal reservoirs defines the permeability patterns and characteristics of each geothermal field. Over past decades, end-member ranges of the permeability patterns have commonly been called *focused* or *fault controlled* for fields where permeability is narrowly confined, and *distributed* over relatively broad areas where permeability is broadly distributed and associated with primary permeability of lithologies or where lithologies host high density of open fractures. Some fields have components of both focused and distributed permeability and have been the subject of further classifications in recent publications. Libbey and Murphy (2026) categorized the *permeability regime* of a convective systems according three categories: *discrete, limited distribution, and enhanced distribution*. Wallis et al. (2017) classified convective systems based on geometries: *focused flow, influenced flow, unconstrained flow*.

Some of the many published case studies that capture elements of these permeability patterns noted above are described in this paragraph. Systems that have upflows hosted in rock types with intrinsically low bulk permeability (i.e., <1 mD), such as the siliciclastic metasedimentary sequences and plutonic rocks common to many systems of the western US Basin and Range, often have relatively small, focused upflow areas that are controlled by local zones of structural complexity, as described above. Conversely, thick young volcanic sequences with heterogeneous rock properties, such as copiously jointed/fractured lavas and welded/propylitically altered pyroclastics, are more commonly associated with elevated bulk permeability (i.e., ~50 to >100 mD) and host large convective systems that approach the unconstrained endmember of Wallis et al., ibid). The lava and ignimbrite sequences at Miravalles, Costa Rica (Zúñiga et al., 2005) and the Reporoa Group at Rotokawa (Milicich et al., 2021) are examples of lithologic units resulting in such relatively broad unconstrained reservoir geometries. Geological mapping is a foundational tool to provide insight into the distribution of subsurface lithologies with varying permeability characteristics. The resulting interpretations portrayed in cross-sections and 3D geological models can hence inform resource area/boundary definitions, fluid flow paths, and temperature contours in geothermal conceptual models.

Reservoir hydrology can be shaped by the subsurface distribution of lithologies with contrasting bulk permeability characteristics, resulting in reservoirs with influenced geometry with focused permeability or combined zones of influenced and unconstrained geometries (Wallis et al., 2017) with different sectors of the reservoir having either locally focused or distributed permeability characteristics. The field identification of lithologies, unit offsets, and intrusive margins that result in the juxtaposition of units with varying bulk permeability characteristics are thus key inputs to geothermal conceptual models. The variation in permeability between lithologies can be primary, secondary, or primary+secondary. Examples of lithologies impacting influenced flow reservoir geometries are the serpentinized ultramafics at Leyte, Philippines (Caranto and Jara, 2015), the greywacke at Broadlands-Ohaaki, New Zealand (Mroczek et al., 2016), and the marine sediments that focus the deep upflow below the unconstrained production reservoir hosted in younger volcanics at Awibengkok, Indonesia (Stimac et al., 2008).

Similarly, permeable volcanic lithologies can also facilitate pathways for pronounced outflows, such as those in Roseau Valley, Dominica (Libbey et al., 2024), Mammoth, USA (Johnson et al., 2022), and Ribeira Grande, Azores (Franco et al., 2018). Permeable buried sedimentary sequences can also host notable outflows, such as the Permian sandstones and dolomites at Cove Fort, Utah (Rowley et al., 2013). Shallow outflows from US Basin and Range geothermal systems are commonly channeled in Neogene basin sediments, often just below the water table, as shown in Figure 4, which illustrates the San Emidio field (Folsom et al., 2020). Other examples are reported at the Hawthorne (Ayling and Hinz, 2020) and Dixie Meadows (Delwiche et al., 2023) fields. Many of these outflows are hosted in silicified sediments and/or silicified volcanics that often do not outcrop. Although silicification sometimes reduces permeability, in zones with active faulting, secondary fracturing of the brittle salified zone can result in very high permeability zones, like at San Emidio (Folsom et al., 2020), Blue Mountain (Fercho et al., 2023), Don Campbell (Kraal et al., 2025), and Humboldt House (Johnson, 2005; Davis, 2011). Such concealed silicified sediments have often been initially identified by drilling but can be inferred pre-drilling through evaluation of gravity and geological map data (e.g., Folsom et al., 2020). Permeability associated with unconformities can also sometimes host outflows, such as at Bweengwa, Zambia (Hinz et al., 2020). The outflow along these unconformities is associated with a combination of factors that contribute to the permeability contrast, including primary and/or secondary clays in the capping unit and potential for high degree of fractures associated with paleo-weathering along the unconformity. Although gravity can detect silicified zones in sediments and MT resistivity can image the smectite clays that cap both the silicified zones and unconformities

associated with outflows of geothermal systems, the design and interpretation of these surveys depend on the initial context provided the geological mapping.

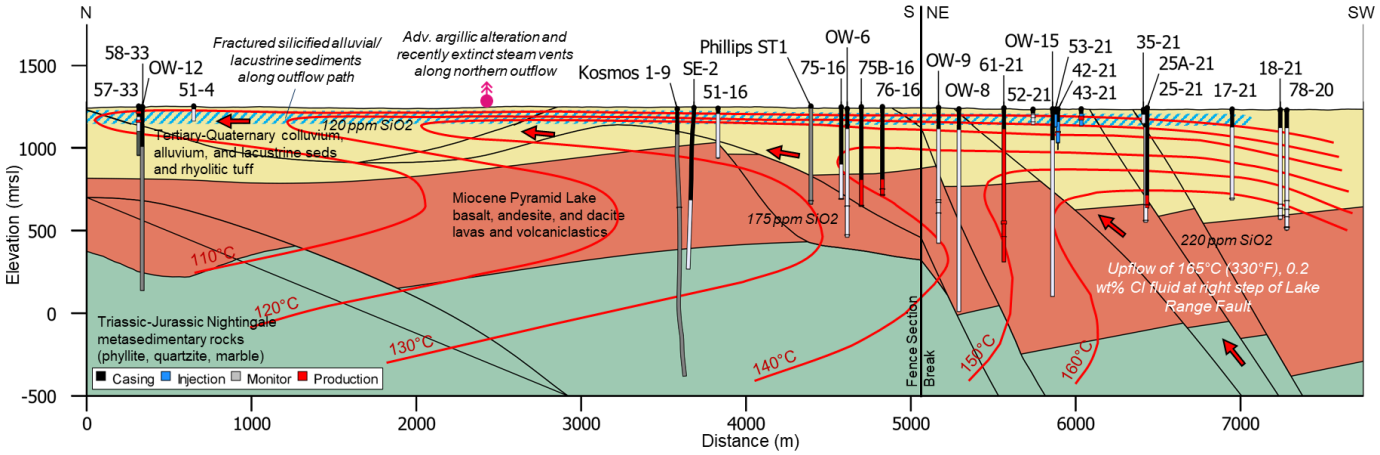


Figure 4: Fence-section of the conceptual model of the San Emidio geothermal system, Nevada, displaying the stratigraphic control of the north-directed shallow outflow, which is shown by red arrows and the isotherm geometry (Folsom et al., 2020).

The primary and dissolution porosity of sedimentary units is the dominant source of permeability in most sedimentary basin-hosted geothermal resources. Where not disrupted by locally permeable structural zones, intercalated clay-rich intervals in the sedimentary package serve as aquicludes/aquitards to limit vertical permeability within sedimentary sequences. This limited vertical permeability is evidenced by the dominantly conductive temperature profiles of geothermal systems in the Imperial Valley (Ramirez et al., 2023) and Pannonian Basin (Horváth et al., 2015). While these environments are characterized by low topography and limited outcrops, surface geological mapping in the (perhaps distal) uplifted ranges surrounding these sedimentary basins can nonetheless provide insight into the stratigraphy and corresponding permeability targets within the basin.

3.4 Lithological/Volcanic Features Related to Marginal Recharge

Geothermal conceptual models require the characterization of both *hot water* and *cold water* hydrology, and it is common that the latter is often as influential on the overall geothermal system geometry. Geological mapping commonly provides important constraints on sources of cold water recharge and identifies features associated with higher risk that cold water might have cooled the reservoir. The geological structures described in Section 3.2 affect permeability that influences the movement of cold water as well as hot water However, there are additional geological features related to stratigraphic permeability and volcanic features that are more commonly associated with the cold-water hydrology of geothermal systems.

Features of geological maps that are commonly associated with cooling the underlying geothermal reservoirs include young monogenetic volcanic features such as domes, maar craters, and scoria cones and their associated conduits, which can sometimes represent zones of pronounced cool recharge into geothermal systems. This is more likely if these features are situated above thin caps or “breaks” in the clay cap of a system that correspond with higher resistivity zones within the low resistivity cap imaged using MT resistivity. Such reservoir-scale downflows can be a natural-state hydrological phenomenon, such as that documented at the Ijen geothermal field in Indonesia (Libbey et al., 2026), Olkaria (Axelsson et al., 2017; Figure), and Aluto Langano (Samrock et al., 2023 and Sisay, 2016), or one that originates from production-induced reservoir pressure drawdown as occurred at Ohaaki, New Zealand (Rissmann et al., 2011), and Tiwi, Philippines (Gambill and Beraquit, 1993). The mapping of such monogenetic features can therefore help identify influences on the system’s hydrology that are relevant to exploration/development strategies and the quantification of project risks.

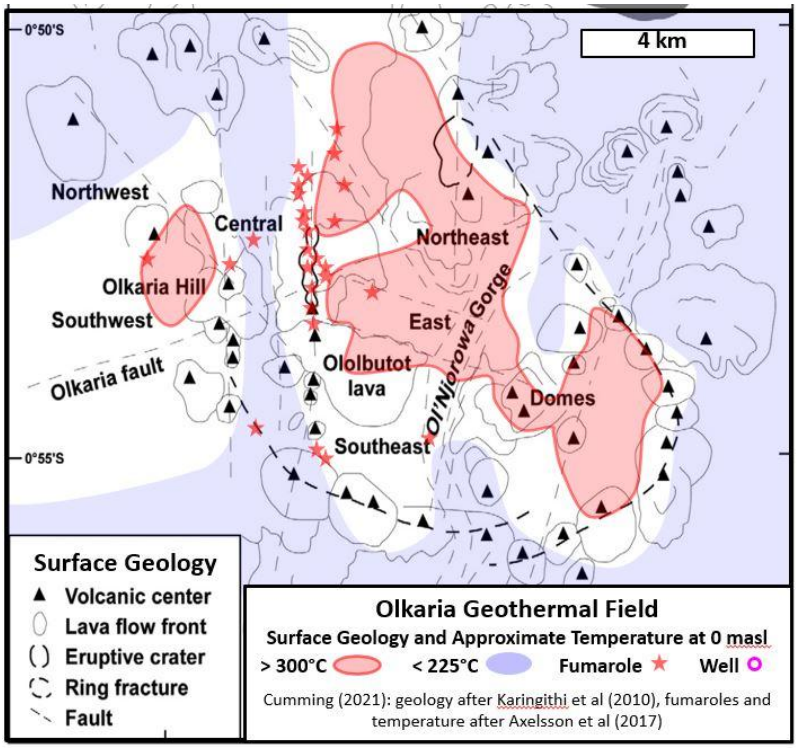


Figure 5: Temperature distribution and geological features of the greater Olkaria geothermal system, Kenya, illustrating the influence of the monogenetic volcanic centers on the cold-water hydrology within the caldera (after Axelsson et al., 2017 and Karingithi et al. 2010).

Additionally, permeable volcanic and sedimentary lithologies can provide stratigraphic pathways for marginal recharge to influence the isotherms/hydrology of geothermal systems. The influx of surface water from Lago de Amatitlan along permeable volcanic stratigraphy and into the Amatitlán geothermal system in Guatemala is one such example (Lima et al., 1996). Permeable carbonate sequences have been hypothesized to channelize the cold-water hydrology of some systems in the Menderes Graben, Turkey, however, there is a paucity of publicly available literature to reference as conclusive analogs for this phenomenon.

3.5 Insights Into Reservoir Chemistry from Geological Mapping

Reservoir lithology inferred from geologic mapping can have a major impact on reservoir fluid composition among other geothermal system characteristics (e.g. temperature, source water, water/rock ratios). This early-stage insight into reservoir geochemical parameters can guide development strategies and the understanding of resource risk. For instance, geologic data on reservoir lithology and water/rock interaction can sometimes inform the likelihood of encountering high-gas reservoir fluids, a variable that can influence whether a medium-temperature field is developed with production pumps or self-flowing wells. Similarly, insight into the potential for high-salinity reservoir fluids from the geologic setting of a geothermal system identified during mapping can flag scaling and corrosion risks early in the exploration stage of a project – parameters that can drastically impact the operational costs of a future development. Pre-drilling insight from geologic mapping can also help with the early-stage interpretation of thermal spring chemistry, e.g., by providing guidance to the question of whether low-TDS, Na-HCO_3 compositions are likely to represent a deep reservoir fluid, conductively or steam-heated groundwater, or a more complex mixture of fluids.

The chemistry of geothermal reservoir fluids is the product of temperature-dependent water-mineral reactions, source fluid compositions (e.g., meteoric vs. seawater vs. connate water), degree of magmatic volatile input, and the chemistry and alteration susceptibility of the host rock. The primary influence of the host rock on the fluid chemistry is the anion budget (Cl, HCO_3, and SO_4), the dissolved gas concentration, silica and major cations (Ca, Na, K, Mg). Since Cl is unbuffered by hydrothermal minerals under most conditions, it can serve as an especially useful indicator of host rock (or fluid source) compositions. When evaporites have influenced the ground water in an area, expectations for geothermal chemistry significantly change, with further analysis required to distinguish the local evaporite composition. To illustrate the correlation of rock-type with reservoir chemistry, the following examples focus on trends identified in liquid-dominated fields with relatively homogenous lithologies and no complicating influences from seawater, evaporites or elevated magmatic volatile inputs. While reservoir temperatures and water-rock ratios influence the fluid chemical composition

through mineral-water reactions and their kinetics, the broad trends discussed here are often relevant in low-, medium-, and high-temperature systems, as illustrated by the diversity of examples provided below.

Liquid-dominated geothermal systems hosted dominantly in intermediate to felsic volcanics generally have 1000-3000 ppm Cl and low to moderate dissolved NCG concentrations, typically between 0.05-0.5 wt%. Many volcanic-hosted geothermal fields around the world share these broad chemical characteristics, such as in the Taupo Volcanic Zone (e.g., Wairakei and Ngatamariki; Giggenbach, 1995), the Sunda Arc (e.g., Ijen; Libbey et al., 2026), the Lesser Antilles Arc (e.g., Roseau Valley; Libbey et al., 2024), and the Central American Volcanic Arc (e.g., Amatitlan and Berlin; Ormat unpublished data; Ruggieri et al., 2010). Systems hosted dominantly in granitoid rocks also tend to share similar Cl and dissolved gas characteristics, e.g., Steamboat, Patua, and Roosevelt in the USA (Ormat unpublished data; Cladouhos et al., 2017; Simmons et al., 2015), Yangbajain in China (Ping et al., 2000), and Zunil in Guatemala (Johnson et al., 2025).

Among the most explicit correlations between host-rock composition and reservoir fluid chemistry is the association of carbonate-rich stratigraphy (e.g., limestones, dolomites, marls, and marbles) with high-gas (CO_2) reservoirs. Dissolved NCG concentrations in such reservoirs commonly range between 1-5 wt%, as has been encountered in the carbonate-rich reservoirs of the Menderes Graben, Turkey (e.g., Kizildere and Alaşehir) and the Tyrrhenian Magmatic Zone in Italy (e.g., Monte Amiata; Haizlip et al., 2013).

Geothermal systems hosted predominantly in basalt or siliciclastic metasediments (e.g., phyllites and quartzites) and no influence of seawater or evaporites show some variability in Cl concentrations but frequently have very low Cl and low to very low dissolved gas concentrations. The Cl-deficient character of these fluids may relate to the low Cl concentrations of most basaltic volcanic glass (e.g., Arnórsson and Andréstóttir, 1995) and siliciclastic metasedimentary rocks. The reservoir fluids of basaltic systems commonly have <100-200 ppm Cl and a Na-Cl character, e.g., Nesjavellir and Hellisheiði (Ármannsson, 2016), Theistareykir (Saby et al., 2022) and Neal Hot Springs in the USA (Murphy et al., 2020). Liquid dominated, non-volcanically heated systems where magmatic gases are not influencing fluid chemistry and are hosted within siliciclastic metasediments are commonly <150 ppm Cl with HCO_3^- (or less-commonly SO_4^{2-}) as the major anionic species. Tuscarora and Beowawe in the USA (Kluge et al., 2025; Cole and Ravinsky, 1984), Platanares and Azucualpa in Honduras (Barberi et al., 2013), and Joaquina in Guatemala (Libbey et al., 2015) are examples of such siliciclastic metasedimentary-hosted systems.

Systems hosted in sedimentary basins can have a vast range of reservoir fluid chemistries. For example, chloride and dissolved gas concentrations, which can vary laterally and vertically throughout the basin, as the limited vertical permeability inherent to many of these settings can impede fluid homogenization by convection and serve to compartmentalize reservoirs. The interaction of subsurface fluids with evaporite sequences in the basin and the influence of connate fluids can result in hypersaline geothermal reservoirs in these settings, where Cl concentrations can exceed 100,000 ppm. Examples of sedimentary basin systems with geothermal fluids that span a wide range of Cl and dissolved gas r include those in the basins of Germany (e.g., Groß Schönebeck and Neustadt-Glewe; Regenspurg, 2012; Seibt et al., 2005), Pannonian Basin (e.g., Velika Ciglena and Bad Blumau; Predovan and Blecich, 2021; Goldbrunner, 2005), and the Imperial Valley (e.g., Salton Sea, Heber, East Mesa, and Brawley; Ramirez et al., 2023).

Information from surface geological mapping can also provide insight into the broad pH conditions of the subsurface. For instance, the identification of solfataras, superheated fumaroles, hyperacidic lakes, and acid-sulfate thermal manifestations surrounded with or without highly altered clays and recent volcanic activity can aid in the delineation of acid vapor cores. However, the presence of sulfurous acid thermal features does not require an acid reservoir fluid alone as such features can originate when steam and gas from boiling of a neutral NaCl fluid separation and flow up separately creating often acidic steam and gas surface manifestations. Conversely, altered clasts incorporated within the ejected material of hydrothermal or phreatic eruptions can provide insight into the existence of a neutral pH system at depth, e.g., clasts containing epidote and calcite. The identification of geologically recent fault zone silicification, calcification, or argillic to propylitic mineralization can also provide insight into the possibility of neutral pH conditions at depth.

3.6 Insights Into Heat Sources from Geological Mapping

Surface mapping and the understanding of the regional geological context for a system (as discussed in Section 3.1) can provide insight into whether proximal, deep/distal, and/or waning magmatic heat sources are conceivable or likely at a geothermal prospect. Indications may be conspicuous, such as for systems situated on the flanks of Holocene stratovolcanoes, e.g., the Momotombo geothermal field in Nicaragua (Porras and Itoi, 2006), adjacent to compositionally-evolved Holocene lava dome and cone features, e.g., the Kawerau

geothermal field, New Zealand (Milicich et al., 2016), or within active volcanic rifts with recent basaltic lava flows, e.g., the Reykjanes geothermal fields in Iceland (Franzson et al., 2002). Most surface characteristics of volcanoes such as the size of each volcanic edifice, the presence and number of domes and other flank vents, average erupted composition or compositional diversity do not have a direct correlation to the presence of geothermal activity, however, a volcano's age does have a correlation, with the majority of geothermal systems (and installed power) in volcanic arcs worldwide being hosted by volcanic centers with eruptions within the past 1000 years (Stelling et al., 2016).

The existence of residual magmatic heat can be more ambiguous at geothermal fields where surface manifestation activity is limited/weak and the youngest volcanic products are Pleistocene in age. Nonetheless, the mapping and identification of eruptive ages as Middle to Late Pleistocene is a positive indication for the potential of residual magmatic heat, especially if the mapped volcanic products are reflective of fractionated upper crustal magma chambers. Examples of geothermal systems that lack Holocene volcanic products, only display weak thermal manifestations, and that had unclear associations to magmatic heat sources prior to drilling include the Domo San Pedro geothermal field in Mexico, with its associated Late Pleistocene dacite domes (Reyes-Orozco et al., 2019), and the Apas Kiri geothermal system in Malaysia, which occurs in association with the waning and eroded Late Pleistocene Mt. Maria stratovolcano (Libbey et al., 2017).

The presence of Holocene to Middle Pleistocene basaltic monogenetic volcanoes at a geothermal prospect is weakly correlated with a shallow magmatic heat source, as these features are typically related to lower crustal magma chambers connected to the surface along narrow dikes that rapidly lose their heat after emplacement (Wohletz and Heiken,1992). While these young mafic monogenetic features cannot conclusively link geothermal activity to a magmatic heat source, they are often associated with regions of thinned lithosphere and related elevated background heat flow values. The lack of magmatic heat source at the Soda Lake geothermal system in Nevada, USA, where there is an adjacent Holocene maar crater (McLachlan et al., 2011), is an example of an amagmatic geothermal system in close proximity to young monogenetic volcanism. Another similar example is provided by the Katwe geothermal system in Uganda (Isabirye, 2018, 2020).

4 INTEGRATING INSIGHTS FROM SURFACE GEOLOGICAL MAPPING INTO EXPLORATION AND DEVELOPMENT WORKFLOWS

Geological maps, cross-sections, and 3D models developed from surface mapping data and interpretations must be integrated with other available geoscientific and downhole data to ensure consistent interpretations of overall stratigraphy, depth of lithological contacts, and fault occurrences/offsets/geometries. For example, geophysical maps and models, such as MT resistivity images and 3D models, gravity maps and models, Bouguer gravity horizontal gradient maps, and RTP total intensity magnetic residual and gradient maps can be useful for identifying buried offsets when the stratigraphy contains units with contrasting physical properties (e.g., conductivity, density, and magnetic susceptibility), such as commonly the case for the alluvial-basement rock juxtaposition in Basin and Range-type settings (Peacock et al., 2018; Folsom et al., 2020; Siler et al., 2020; Delwiche et al., 2023; Wiggins et al., 2025). Seismic data, while not utilized as ubiquitously in geothermal as in hydrocarbon exploration, can sometimes support surface mapping where it can image stratigraphic offsets, folding, and the basement rock depth in sedimentary or mixed sedimentary-volcanic environments (Queen et al., 2016). Most importantly, maps and cross-sections generated from surface geological mapping must also be integrated with available well data such as lithological logs, feedzone distributions, borehole image logs, petrophysical logs, and litho-geochemistry data (Milicich et al., 2018; Ikhwan et al., 2021; Wallis et al., 2023; Libbey and Williams-Jones, 2015). Wellbore interference tests, tracer studies, and pressure/temperature distributions can also provide information pertaining to permeability pathways and reservoir compartments that should be contextualized within the broader geological model of the subsurface.

A critical tool in any geothermal development is a numerical reservoir model, which is generally constructed once a resource confirmation well has been drilled and there is sufficient well testing data to facilitate calibration. This tool enables reservoir forecasting and can help inform development strategies, such as the targeted project capacity and the optimization of injection and production configurations. Information from the geological model allows for an understanding of the subsurface that extrapolates beyond the available narrow well constraints. Thus, it is imperative that geologists collaborate with the numerical modeling specialist to provide insight into the division and geometry of permeability units in the model and to provide input for other system attributes such as the water table elevation and the location/type/temperature/flux of surface manifestations (Nugraha et al., 2022; Murphy, 2026). The permeability model should consider insight into lithological-, fault/fracture-, volcanological- (e.g., diatremes, dikes, and domes), and alteration-based influences on the permeability of the subsurface. It may also be important to specifically delineate aquitards or

aquicludes that vertically compartmentalize the reservoir; features that are especially relevant for systems with under pressured or overpressure pore space conditions.

Geological models also provide the foundation for further stress field and slip and dilation tendency modeling, which can help contextualize the structural setting and distribution of fracture permeability within a geothermal system. An example of this is the stress-transfer modeling of Siler (2023) and Melosh (2026), which utilize boundary element methods to model fault slip and the corresponding distribution of crustal stress and strain across a geothermal field. An additional method is the use of slip and dilation tendency, which describes the likelihood of a fracture to shear under a given stress tensor, and whether that shear will enhance or reduce fracture porosity and permeability. Modeling slip and dilation tendency for mapped faults (Ferrill et al., 2020; Siler, 2022) and fractures from borehole image logs (Wallis, 2023) can identify which structural attitudes are optimally oriented to facilitate fracture-based permeability. Investigations of borehole breakouts and drilling induced tensile fractures in image logs can also reveal local stress field rotations related to structural discontinuities (Fercho et al., 2020, 2023; Wallis et al., 2023; Libbey et al., 2026). Synergies between stress field calculations between surface measurements from fault surfaces and borehole data have been demonstrated in multiple geothermal areas (Hinz et al., 2010, 2016; Blake, 2011; Blake and Davatzes, 2012; Blake et al., 2015; Jolie et al., 2015; Ayling and Hinz, 2020) The integration of these modeling methods with the results of surface geological mapping constitutes powerful, and currently underutilized, workflows for enhancing the structural understanding of geothermal systems.

5 CONCLUSIONS

Geological mapping is central to developing geothermal conceptual models. Many geologic map-derived insights are transferable across geologic settings and demonstrate the utility of selecting analogues from a broad range of settings and temperature regimes. Analysis priorities for convective geothermal systems always include identifying possible upflow and outflow patterns as well as implications for cold water hydrology and marginal recharge. Aside from the identification of the structural framework and lithologies of a system, specific emphasis for volcanic systems is placed on identifying gaps in the continuity of smectite cap (e.g., mapping of domes or localized exposures of high rank alteration) and areas that could host cool downflow (e.g., a major fault zone exposed in brittle bedrock). Emphasis for non-volcanic deep circulation systems includes assessing recharge and cooling risks from nearby mountain ranges where brittle permeable lithology may be exposed, as well as gleaning insight into the chemical composition of the reservoir, which can be influenced by the host lithologies and adjacent rocks, like evaporites, issues that have implications for project risk and development strategies. EGS projects focus on identifying simpler structural areas with stress fields that can be predictable over relatively large areas. For all projects, volcanic, deep circulation, and EGS projects, iterative integration of mapping, modeling, and operational data improves the predictive value of conceptual models. Future work and publications could involve further standardized mapping-to-model workflows, building analogue databases, and improvements on the workflow to integrate geological data with geophysical datasets, stress inversion models, and numerical reservoir models.

REFERENCES

Ármannsson, H. (2016). The fluid geochemistry of Icelandic high temperature geothermal areas. Applied Geochemistry, 66, 14–64.

Arnórsson, S. and Andréstóttir, A., (1995). Processes controlling the distribution of boron and chlorine in natural waters in Iceland. Geochemica et Cosmochimica Acta, 59(20), p. 4125-4146.

Axelsson, G., Gudmundsdóttir, V., Arnaldsson, A., Ármannsson, H., Árnason, K., Einarsson, G., Franzson, H., Halldórsdóttir, S., Hersir, G., Kamunya, K., Níelsson, S., Okoo, J., Omiti, A., Ouma, P., (2017). Revision of the Conceptual Model for the Olkaria Geothermal System, Kenya. Proc. Stanford Geotherm. Work. 1–9.

Ayling, B. F., and Hinz, N. H. (2020). Developing a conceptual model and power capacity estimates for a low-temperature geothermal prospect with two chemically and thermally distinct reservoir compartments, Hawthorne, Nevada, USA. Geothermics, 87, 20 p.

Barberi, F., Carapezza, M. L., Cioni, R., Lelli, M., Menichini, M., Ranaldi, M., Ricci, T., and Tarchini, L. (2013). New geochemical investigations in Platanares and Azacualpa geothermal sites (Honduras). Journal of Volcanology and Geothermal Research, 257, 113–134.

Barton, C. A., Zoback, M. D., and Moos, D. (1995). Fluid flow along potentially active faults in crystalline rock. Geology, 23, 23–27. doi:10.1130/0091-7613(1995)023<0683.

Bell, J. W., and Ramelli, A. R. (2007). Active faults and neotectonics at geothermal sites in the western Basin and Range: Preliminary results. GRC Transactions, 31, 375–378.

Blake, K. (2011). HWAAD-2A and HWAAD-3: Fracture and Stress Analysis, Hawthorne Army Depot, Hawthorne, NV: Initial Assessment. Internal Navy Geothermal Program Office Technical Report, 18 p.

Blake, K., and Davatzes, N. C. (2012). Borehole image log and statistical analysis of FOH-3D, Fallon Naval Air Station, NV. Proceedings, Thirty-Seventh Workshop on Geothermal Reservoir Engineering, Stanford University, 1054–1067.

Blake, K., Tiedeman, A., Sabin, A., Lazaro, M., Meade, D., and Huang, W.-C. (2015). Naval Air Station Fallon Mainside: Update of geothermal exploration. Geothermal Resources Council Transactions, 39, 407–414.

Bouchot, V., Sanjuan, B., Traineau, H., Guillou-Frottier, L., Thinon, I., Baltassat, J. M., Fabriol, H., Bourgeois, B., and Lasne, E. (2010). Assessment of the Bouillante geothermal field (Guadeloupe, French West Indies): Toward a conceptual model of the high temperature geothermal system. Proceedings, World Geothermal Congress, 8 p.

Brogi, A. (2008). Fault zone architecture and permeability in siliceous sedimentary rocks: Insights from the Rapolano geothermal area (Northern Apennines, Italy). Journal of Structural Geology, 30, 237–256.

Caine, J. S., Evans, J. P., and Forster, C. B. (1996). Fault zone architecture and permeability structure. Geology, 24(11), 1025–1028.

Caranto, J. A., and Jara, M. P. (2015). Factors controlling reservoir permeability at the Leyte geothermal field, Philippines. Proceedings, World Geothermal Congress, 8 p.

Carver, C., Brown, Z., Haizlip, J., and Casteel, J. (2021). Geochemical modeling for reservoir characterization, wellfield development, and power plant design for the Star Peak geothermal reservoir in Rye Patch, Nevada, USA. GRC Transactions, 45, 950–958.

Cladouhos, T. T., Uddenberg, M. W., Swyer, M. W., Nordin, Y., and Garrison, G. H. (2017). Patua geothermal geologic conceptual model. GRC Transactions, 41, 19 p.

Cole, D. R., and Ravinsky, L. I. (1984). Hydrothermal alteration zoning in the Beowawe geothermal system, Eureka and Lander Counties, Nevada. Economic Geology, 79, 759–767.

Craig, J. W., Klemperer, S. L., Crossey, L. J., Karlstrom, K. E., and Zhao, P. (2024). Preliminary tectonic and structural controls of geothermal springs of the Tibetan Plateau: Insight from regional-scale sampling of helium isotopes (3He/4He), stable isotopes, and aqueous geothermometry. Proceedings, 49th Workshop on Geothermal Reservoir Engineering, Stanford University, Stanford, California, February 12–14, 2024, SGP-TR-227, 18 p.

Curewitz, D., and Karson, J. A. (1997). Structural settings of hydrothermal outflow: Fracture permeability maintained by fault propagation and interaction. Journal of Volcanology and Geothermal Research, 79, 149–168.

Davis, D. A. (2011). Descriptive logs, skeletonized samples, and photographs of core from Presco Energy's thermal gradient wells P 3-1, P 10-1, and P 32-2 in the Rye Patch Area, Pershing County, Nevada. NBMG Open-File Report 2011-10, 2 p. (with online sample descriptions and photographs).

Delwiche, B., Libbey, R., Folsom, M., Johnson, A., Murphy, J., Zuza, R., Reno, P. S., and Usa, N. (2023). Exploration history and conceptual model of the Dixie Meadows geothermal field, Nevada, USA. Proceedings, World Geothermal Congress 2023, 19 p.

Fairley, J. P., and Hinds, J. J. (2004). Rapid transport pathways for geothermal fluids in an active Great Basin fault zone. Geology, 32(9), 825–828.

Faulds, J.E., Hinz, N. H., Hannah Giddens, M., Chambefort, I., Coolbaugh, M. (2026). Favorable structural settings of geothermal systems in active tectonic regions: A global perspective. Proceedings, WGC 2026 (this volume).

Faulds, J. E., and 6 others (2010). Structural controls of geothermal activity in the northern Hot Springs Mountains, western Nevada: The tale of three geothermal systems. Geothermal Resources Council Transactions, 34, 675–683.

Faulds, J. E., Bouchot, V., Moeck, I., and Oguz, K. (2009). Structural controls on geothermal systems in western Turkey: A preliminary report. Geothermal Resources Council Transactions, 33, 375–381.

Faulds, J. E., Coolbaugh, M. F., and Hinz, N. H. (2021). Inventory of structural settings for active geothermal systems and late Miocene (~8 Ma) to Quaternary epithermal mineral deposits in the Basin and Range Province of Nevada. Nevada Bureau of Mines and Geology Report 58, 27 p., 3 plates, scale 1:2,500,000.

Faulds, J. E., Coolbaugh, M. F., Vice, G. S., and Edwards, M. L. (2006). Characterizing structural controls of geothermal fields in the northwestern Great Basin: A progress report. Geothermal Resources Council Transactions, 30, 69–76.

Faulds, J. E., Hinz, N. H., and Kreemer, C. W. (2012). Regional patterns of geothermal activity in the Great Basin Region, western USA: Correlation with strain rates. Geothermal Resources Council Transactions, 36, 897–902.

Faulds, J. E., Hinz, N. H., Coolbaugh, M. F., Cashman, P. H., Kratt, C., Dering, G., Edwards, J., Mayhew, B., and McLachlan, H. (2011). Assessment of favorable structural settings of geothermal systems in the Great Basin, Western USA. Geothermal Resources Council Transactions, 35, 777–784.

Faulds, J. E., Hinz, N. H., Dering, G. M., and Siler, D. L. (2013). The hybrid model – the most accommodating structural setting for geothermal power generation in the Great Basin, western USA. Geothermal Resources Council Transactions, 37, 3–10.

Faulds, J.E., Ramelli, A.R., Coolbaugh, M.F., Hinz, N.H., Garside, L, J., and Queen, J.H., (2017). Preliminary geologic map of the Bradys geothermal area, Churchill County, Nevada. NBMG Open-File Report 17-4, 1 sheet, 1:12,000 scale.

Faulds, N. H., and Hinz, N. H. (2015). Favorable tectonic and structural settings of geothermal systems in the Great Basin Region, western USA: Proxies for discovering blind geothermal systems. Proceedings, World Geothermal Congress 2015, Melbourne, Australia, 6 p.

Faulds, N. H., Hinz, N. H., dePolo, C., Hammond, W., Kreemer, C., Shevenell, L., Queen, J., Siler, D., Visser, C., and Wannamaker, P. (2015). Discovering blind geothermal systems in the Great Basin region: An integrated geologic and geophysical approach for establishing geothermal play fairways. Final report to the U.S. DOE, 110 p.

Fercho, S., Hinz, N., Casteel, J., and Turk, J. (2020). Analysis of natural and drilling induced fractures from newly acquired borehole image logs at the Star Peak geothermal field, NV: Implications for localized stress field rotation within a normal fault step-over. GRC Transactions, 44, 557–571.

Fercho, S., Norbeck, J., McConville, E., Hinz, N., Wallis, I., Titov, A., Agarwal, S., Dadi, S., Gradl, C., Baca, H., Eddy, E., Lang, C., Voller, K., and Latimer, T. (2023). Geology, state of stress, and heat in place for a horizontal well geothermal development project at Blue Mountain, Nevada. Proceedings, 48th Workshop on Geothermal Reservoir Engineering, 16 p.

Ferrill, D. A., Smart, K. J., and Morris, A. P. (2020). Resolved stress analysis, failure mode, and fault-controlled fluid conduits. Solid Earth, 11(3), 899–908.

Folsom, M., Libbey, R., Feucht, D., Warren, I., and Garanzini, S. (2020). Geophysical observations and integrated conceptual models of the San Emidio geothermal field, Nevada. 21 p.

Franco, A., Guimarães, T., and Henneberger, R. (2018). Geothermal geology of the outflow zone of the Ribeira Grande geothermal system. GRC Transactions, 42, 1316–1326.

Franzson, H., Thordarson, S., Bjornsson, G., Gudlaugsson, S. T., Richter, B., Fridleifsson, G. O., and Thorhallsson, S. (2002). Reykjanes high-temperature field, SW-Iceland: Geology and hydrothermal alteration of well RN-10. Proceedings, Twenty-Seventh Workshop on Geothermal Reservoir Engineering, 8 p.

Gambill, D. T., and Beraquit, D. B., Development history of the Tiwi geothermal field, Philippines, in Geothermics Special Issue on Geothermal Systems in the Philippines, D. Sussman (ed.), Volume 22, Issue 5, p. 403-416.

Giggenbach, W. F. (1995). Variations in the chemical and isotopic composition of fluids discharged from the Taupo Volcanic Zone, New Zealand. Journal of Volcanology and Geothermal Research, 68(1–3), 89–116.

Goldbrunner, J. (2005). Bad Blumau (Styria, Austria)—The success story of combined use of geothermal energy. GHC Bulletin, 27–30.

Haizlip, J. R., Haklidir, F. T., and Garg, S. K. (2013). Comparison of reservoir conditions in high noncondensible gas geothermal systems. 12 p.

Hinz, N. H., Coolbaugh, M., Faulds, J. E., Shevenell, L., and Stelling, P. (2016a). Regional quantitative play fairway analysis: Methodology, global examples, and application for the East African Rift System. Proceedings, 6th African Rift Geothermal Conference, Addis Ababa, Ethiopia, 2–4 November 2016, 12 p.

Hinz, N. H., Coolbaugh, M., Shevenell, L., Melosh, G., Cumming, W., and Stelling, P. (2016b). Structural–tectonic settings for globally productive subduction arc volcanic centers. Proceedings, 41st Workshop on Geothermal Reservoir Engineering, Stanford University, Stanford, CA, February 22–24, 8 p.

Hinz, N. H., Cumming, B., and Sussman, D. (2018). Exploration of fault-related deep-circulation geothermal resources in the western branch of the East African Rift System: Examples from Uganda and Tanzania. Proceedings, 7th African Rift Geothermal Conference, Kigali, Rwanda, 31 October – 2 November 2018, 16 p.

Hinz, N. H., Faulds, J. E., and Coolbaugh, M. F. (2014). Association of fault terminations with fluid flow in the Salt Wells geothermal field, Nevada, USA. Geothermal Resources Council Transactions, 38, 3–9.

Hinz, N. H., Faulds, J. E., Moeck, I., Bell, J. W., and Oldow, J. S. (2010). Structural controls of three blind geothermal resources at the Hawthorne Ammunitions Depot, west-central Nevada. Geothermal Resources Council Transactions, 34, 785–790.

Hinz, N. H., Matson, G., Sussman, D., Haizlip, J., Turk, J., Carver, C., Fercho, S., Hendri, R., Siagian, H., Fishbin, A., Cumming, W., Letvin, A., and Milton, A. (2021). Conceptual model update of the Sorik Marapi geothermal prospect, Sumatra, Indonesia. GRC Transactions, 45, 2225–2242.

Hinz, N. H., Milton, A., Cumming, W., and Faulds, J. E. (2024). Geological mapping standards for developing geothermal resource conceptual models: Survey design, applications, pitfalls and remedies. GRC Transactions, 48, 1310–1336.

Hinz, N. H., Vivian-Neal, P., Haizlip, J., Matson, G., Cumming, W., Harrison, P., and Campbell, S. (2020). Zambia: Conceptual model and drilling update of the deep circulation Bweengwa River geothermal prospect. Proceedings, World Geothermal Congress, 16 p.

Hinz, N.H., Cumming, C., Matson, G., Haizlip, J., Sussman, D., Fercho, S., Fishbin, A., Sanjaya, D., Sagala, B., Tang, Y., 2020, Conceptual Model Update of the Sokoria Geothermal Field, Flores, Indonesia: World Geothermal Congress, 12 p.

Horváth, F., Musitz, B., Balázs, A., Végh, A., Uhrin, A., Nádor, A., Koroknai, B., Pap, N., Tóth, T., and Wórum, G. (2015). Evolution of the Pannonian Basin and its geothermal resources. Geothermics, 53, 328–352.

Ikhwan, M., Wallis, I. C., and Rowland, J. V. (2021). Integrated analysis of surface and borehole data to construct the stratigraphy model of Bukit Daun field, Indonesia. Proceedings, World Geothermal Congress, 13 p.

Isabirye, E. M., Cumming, W., Askew, T., Hinz, N., Sussman, D., Mawejje, P., and Lugaizi, I. (2020). The Katwe geothermal prospect in western Uganda: A deep-circulation fault zone-hosted geothermal system. Proceedings, World Geothermal Congress, 14 p.

Isabirye, E. M., Hinz, N., Natukunda, J. F., Mawejje, P., and Lugayizi, I. (2018). Status of geothermal energy exploration at Katwe-Kikorongo geothermal prospect, western Uganda. Proceedings, 7th African Rift Geothermal Conference, Kigali, Rwanda, 31 October – 2 November 2018, 15 p.

Johnson, A., Porras, E., Libbey, R., Orozco, E., Magariño, A. A., and Cohen, G. (2025). Injection-well caustic treatments at Zunil, Guatemala: Learnings and lessons from multiple chemical cleanouts of injection wells R3 and R5. GRC Transactions, 20 p.

Johnson, A., Selwood, R., and Feucht, D. (2022). The Geothermal Geodometer: A geochemical approach to targeting upflow in Long Valley. Proceedings, 47th Workshop on Geothermal Reservoir Engineering, 8 p.

Johnson, J. L. (2005). Characterization of past hydrothermal fluids in the Humboldt House geothermal area, Pershing County, NV: Geochemical and paragenetic studies of core samples. Master's Thesis, University of Nevada, Reno, 243 p.

Jolie, E., Faulds, J. E., and Moeck, I. (2012). The development of a 3D structural-geological model as part of the geothermal exploration strategy – A case study from the Brady's geothermal system, Nevada, USA. Proceedings, 37th Workshop on Geothermal Reservoir Engineering, Stanford University, 421–425.

Jolie, E., Scott, S., Faulds, J., Chambefort, I., Axelsson, G., Gutierrez Negrin, L. C., Regenspurg, S., Ziegler, M., Ayling, B., Richter, A., and Zemedkun, M. T. (2021). Geological controls on geothermal resources for power generation. Nature Reviews Earth and Environment. doi:https://doi.org/10.1038/s43017.

Karingithi, C.W., Arnorsson, S., Gronvold, K., 2010. Processes controlling aquifer compositions in the Olkaria geothermal system, Kenya. Journal of Volcanology and Geothermal Research. 196, 57-76.

Kluge, E.-K., Ferguson, C., Reynolds, Z., Motley, C., Libbey, R., Murphy, J., and Akerley, J. (2025). Updated conceptual model and reservoir assessment of the Tuscarora geothermal field: Over a decade of renewable power generation. GRC Transactions, 24 p.

Kraal, K., Folsom, M., Winn, C., Feucht, D., Delwiche, B., Hinz, N., Cumming, W., Sewell, S., and Downs, C. (2025). Petrologic validation of exploration geophysical anomalies utilizing drill core and cuttings from the Don A. Campbell geothermal system, Nevada, USA. Proceedings, 50th Workshop on Geothermal Reservoir Engineering, Stanford University, Stanford, California, February 10–12, 2025, SGP-TR-229, 18 p.

Libbey, R. B., and Williams-Jones, A. E. (2015). Applications of downhole lithogeochemistry to geothermal exploration. GRC Transactions, 39, 451–463.

Libbey, R. B., Williams-Jones, A. E., Melosh, B. L., and Backeberg, N. R. (2015). Characterization of geothermal activity along the North American–Caribbean Plate boundary in Guatemala: The Joaquina geothermal field. Geothermics, 56, 17–34.

Libbey, R., & Murphy, J. (2026). Standardized definitions and permeability regimes for the characterization and capacity estimation of geothermal systems. Proc. 51st Workshop on Geothermal Reservoir Engineering, 19 p.

Libbey, R., Bogie, I., Peng, W. F., Duasing, J., Payer, A., Lojingau, D., Urzua, L., Ussher, G., and Brotheridge, J. (2017). Insights into the Apas Kiri geothermal system from AK-1D – Malaysia's first geothermal exploration well. GRC Transactions, 41, 1172–1183.

Libbey, R., Murphy, J., John, F., Eloi, D., Webbison, S., Jónsson, S. S., Þorbjörnsson, D., Johnson, A., Bruney, R., Reynolds, Z., Zuza, R., and Spake, D. (2024). Conceptual model of the Roseau Valley geothermal system, Dominica, Lesser Antilles. Proceedings, 46th New Zealand Geothermal Workshop, 10 p.

Libbey, R., Saputra, I., Murphy, J., Husein, M., Dermawan, F., Archady, D., Webbison, S., Novianto, Deuhart, A., Utomo, D., Johnson, A., Spielman, P., Reynolds, Z., Hadi, J., Cumming, W., Marini, L., Parini, M., Rudyawan, A., Wallis, I., and Kurniawan, I. A. (2026). Conceptual model of the Ijen geothermal field, East Java: Indonesia's first developed blind geothermal system. Proceedings, World Geothermal Congress, 12 p.

Lima, E., Fujino, T., McNitt, J. R., Klein, C. W., Greensfelder, R. W., Robertson-Tait, A., Roldan, A., and Palma, J. (1996). A hydrogeological and geochemical model of the high-temperature geothermal system of Amatitlan, Guatemala. GRC Transactions, 347–352.

McLachlan, H. S., Benoit, W. R., and Faulds, J. E. (2011). Structural framework of the Soda Lake geothermal area, Churchill County, Nevada. GRC Transactions, 35, 925–930.

Melosh, B. (2026). Stepovers and beyond: Structural controls of the Geysers geothermal system and the broader Clear Lake region. Proc. 51st Workshop on Geothermal Reservoir Engineering, 10 p.

Micklethwaite, S., and Cox, S. F. (2004). Fault-segment rupture, aftershock-zone fluid flow, and mineralization. Geology, 32(9), 813–816.

Milicich, S. D., Chambefort, I., Simpson, M. P., Wilson, C. J. N., Alcaraz, S., Bardsley, C., and Morales, A. G. (2021). Geology, geochronology, alteration and geochemistry of the Rotokawa geothermal system, Taupō Volcanic Zone, New Zealand. Proceedings, World Geothermal Congress, 12 p.

Milicich, S. D., Clark, J. P., Wong, C., and Askari, M. (2016). A review of the Kawerau geothermal field, New Zealand. Geothermics, 59, 252–265.

Milicich, S. D., Massiot, C., and McNamara, D. D. (2018). Volcanic texture identification and influence on permeability using a borehole resistivity image log in the Whakamaru Group ignimbrite, Wairakei geothermal field, New Zealand. Proceedings, 43rd Workshop on Geothermal Reservoir Engineering, 1–11.

Milton, A., Hinz, N., Fishbin, A., Ammar, A., Lundquist, M., Chandra, V., and Alhani, A., 2023, Exploration for blind, deep circulation, geothermal resources along gulf of Aqaba coastal region of NEOM, Saudi Arabia: GRC Transactions, v. 47, p. 1484-1498.

Mroczek, E. K., Milicich, S. D., Bixley, P. F., Sepulveda, F., Bertrand, E. A., Soengkono, S., and Rae, A. J. (2016). Ohaaki geothermal system: Refinement of a conceptual reservoir model. Geothermics, 59, 311–324.

Murphy, J. F. (2026). Reservoir modeling from exploration to expansion: The Ormat workflow. Proceedings, World Geothermal Congress.

Murphy, J. F., Libbey, R. B., Warren, I., Holt, R. J., Owens, L. B., O'Brien, J., and others (2021). Resource model calibration at Neal Hot Springs, Oregon, USA. Proceedings, World Geothermal Congress 2020, 6 p.

Mussofan, W., Baroek, M. C., Stimac, J., Sidik, R. P., Ramadhan, I., and Santana, S. (2018). Geothermal resource exploration along Great Sumatera Fault segments in Muara Laboh: Perspectives from geology and structural play. Proceedings, 43rd Workshop on Geothermal Reservoir Engineering, SGP-TR-213.

Nugraha, R. P., O'Sullivan, J., O'Sullivan, M., and Abdurachman, F. (2022). Geothermal modelling: Industry standard practices. Proceedings, 47th Workshop on Geothermal Reservoir Engineering, 12 p.

Peacock, J. R., Glen, J., Ritzinger, B., Earney, T., Schermerhorn, W., and Siler, D. (2018). Geophysical imaging of geothermal systems spanning various geologic settings. GRC Transactions, 10 p.

Ping, Z., Ji, D., and Jian, J. (2000). A new geochemical model of the Yangbajing geothermal field, Tibet. Proceedings, World Geothermal Congress, 2007–2012.

Porras, E. A., and Itoi, R. (2006). The Momotombo geothermal system and its conceptual model. GRC Transactions, 33–38.

Predovan, M., and Blecich, P. (2021). Thermodynamic analysis of a 17.5 MW geothermal power plant operating with binary Organic Rankine Cycle. International Scientific Journal "Machines. Technologies. Materials", 2, 49–52.

Ramirez, G., Zuza, R., Johnson, A., Murphy, J., and Akerley, J. (2023). Integrated conceptual model of sedimentary basin-hosted geothermal fields in Imperial Valley, CA. GRC Transactions, 1551–1572.

Rawling, G. C., Goodwin, L. B., and Wilson, J. L. (2001). Internal architecture, permeability structure, and hydrologic significance of contrasting fault-zone types. Geology, 29(1), 43–46.

Regenspurg, S. (2012). Geothermal fluids—Monitoring in Groß Schönebeck. GeoEn Summer School.

Reyes-Orozco, V., Avalos-Tapia, D., Garcia-Tirado, J., Rodriguez-Pineda, E., and Ocampo-Aguilar, F. (2019). Preliminary conceptual model of the Domo San Pedro geothermal field—Western sector of Trans-Mexican Volcanic Belt, Nayarit, Mexico. Proceedings, 44th Workshop on Geothermal Reservoir Engineering, 8 p.

Rissmann, C., Nicol, A., Cole, J., Kennedy, B., Fairley, J., Christenson, B., Leybourne, M., Milicich, S., Ring, U., and Gravley, D. (2011). Fluid flow associated with silicic lava domes and faults, Ohaaki hydrothermal field, New Zealand. Journal of Volcanology and Geothermal Research, 204(1–4), 12–26.

Rowland, J. V., and Sibson, R. H. (2004). Structural controls on hydrothermal flow in a segmented rift system, Taupo Volcanic Zone, New Zealand. Geofluids, 4, 259–283.

Rowland, J. V., and Simmons, S. F. (2012). Hydrologic, magmatic, and tectonic controls on hydrothermal flow, Taupo Volcanic Zone, New Zealand: Implications for the formation of epithermal vein deposits. Economic Geology, 107, 427–457.

Rowley, P. D., Rutledge, E. F., Maxwell, D. J., Dixon, G. L., and Wallace, C. A. (2013). Geology of the Sulphurdale geothermal-resource area, Beaver and Millard Counties, Utah. Open-File Report 609, 33 p.

Ruggieri, G., Dallai, L., Nardini, I., Henriquez, E. T., and Arias, A. (2010). Thermo-chemical variations of the hydrothermal fluids in the Berlin geothermal field (El Salvador). Proceedings, World Geothermal Congress, 7 p.

Saby, M., Hinsberg, V.V., Pinti, D.L., Berlo, K., Gautason, B., Sigurðardóttir, Á., Brown, K., Rocher, O., (2022). The behaviour of metals in deep fluids of NE Iceland. Nature Scientific Reports, 12, Article 21952.

Samrock, F., Grayver, A., Dambly, M. L. T., Müller, M. R., and Saar, M. O. (2023). Geophysically guided well siting at the Aluto-Langano geothermal reservoir. Geophysics, 88(5), 10 p.

Seibt, P., Kabus, F., and Hoth, P. (2005). The Neustadt-Glewe geothermal power plant—Practical experience in the reinjection of cooled thermal waters into sandstone aquifers. Proceedings, World Geothermal Congress, 1–4.

Sibson, R. H. (1994). Crustal stress, faulting and fluid flow. Geological Society, London, Special Publication, 78, 69–84.

Siler, D. (2022). Shapefile for slip tendency and dilation tendency calculated for Quaternary faults in the Great Basin. USGS Digital Object Identifier Catalog.

Siler, D. L. (2023). Structural discontinuities and their control on hydrothermal systems in the Great Basin, USA. Geoenergy, 1, 10 p.

Siler, D. L., Witter, J. B., Craig, J. W., Faulds, J. E., Glen, J. M., Earney, T. E., Schermerhorn, W. D., Peacock, J. R., and Fournier, D. (2020). Using 3D gravity inversion modeling to iteratively refine 3D geologic maps: The Nevada Play-Fairway Project, Southern Gabbs Valley, Nevada. GRC Transactions, 638–656.

Siler, D.L., and Depin, J.D., 2021. 3-D Geologic controls of hydrothermal fluid flow at Brady geothermal field, Nevada, USA. Geothermics, 94, 102112.

Simmons, S., Kirby, S., Moore, J., Wannamaker, P., and Allis, R. (2015). Comparative analysis of fluid chemistry from Cove Fort, Roosevelt and Thermo: Implications for geothermal resources and hydrothermal systems on the east edge of the Great Basin. GRC Transactions, 8 p.

Sisay, S. (2016), Sub-Surface Geology, Hydrothermal Alteration And 3d Modelling Of Wells La-9d And La-10d In The Aluto Langano Geothermal Field, Ethiopia. MSc Thesis. Univ. Iceland. 83 pp.

Stelling, P., Shevenell, L., Hinz, N., Coolbaugh, M., Melosh, G., and Cumming, W. (2016). Geothermal systems in volcanic arcs I: Volcanic characteristics and surface manifestations as indicators of geothermal potential and favorability worldwide. Journal of Volcanology and Geothermal Research, 324, 57–72.

Stimac, J., Nordquist, G., Suminar, A., and Sirad-Azwar, L. (2008). An overview of the Awibengkok geothermal system, Indonesia. Geothermics, 37, 300–331.

Stimac, J., Sihotang, A. M., Mussofan, W., Baroek, M., Jones, C., Moore, J. N., and Schmitt, A. K. (2019). Geologic controls on the Muara Laboh geothermal system, Sumatra, Indonesia. Geothermics, 82, 97–120.

Townsend, J., and Zoback, M. D. (2000). How faulting keeps the crust strong. Geology, 28, 399–402. doi:10.1130/0091-7613(2000)28<399:HFKTCS>2.0.CO.

Wallis, I. C. (2023). The geologic controls on geothermal fluid flux at the district-, reservoir-, and wellbore-scale. PhD thesis, University of Auckland.

Wallis, I. C., Rowland, J. V., Cumming, W., and Dempsey, D. (2017). The subsurface geometry of a natural geothermal reservoir. Proceedings, 39th New Zealand Geothermal Workshop, 9 p.

Wallis, I.C., Milton, A., Brown, Z., Davis, L., Casteel, J., and Peters, B. (2023). Faults, fractures, formation, and stress at Fish Lake: Controls on wellbore-scale permeability in a deep circulation geothermal system. GRC Transactions, 1852–1871.

Wallis, I.C., Moon, H., Clearwater, J., Azwar, L., and Barnes, M. (2015). Perspectives on geothermal permeability. Proceedings, 37th New Zealand Geothermal Workshop, 7 p.

Wiggins, A., Silva, N., Johnson, A., Reynolds, Z., Libbey, R., and Murphy, J. (2025). Successful injection well 85A-18 at the Beowawe geothermal field, Nevada, USA: Implications of high permeability from injection testing. GRC Transactions, 49, 1639–1659.

Wohletz, K., and Heiken, G. (1992). Volcanology and geothermal energy. University of California Press.

Zúñiga, E. V., Rojas, L. C., Víquez, M. B., Zúñiga, F. M., Hakanson, E. C., and Protti, O. M. (2005). Geologic model of the Miravalles geothermal field. Proceedings, World Geothermal Congress, 5 p.